COMPEL: The International Journal for Computation and Mathematics in Electrical and Electronic Engineering

Optimized designing of a patch phased array with a MoM-solver

Yuanhao Wang, Michael Berens, Alexander Nietsch, Werner John, Wolfgang Mathis,

The current issue and full text archive of this journal is available at
www.emeraldinsight.com/0332-1649.htm

SELECTED PAPER

Optimized designing of a patch phased array with a MoM-solver

Yuanhao Wang, Michael Berens and Alexander Nietsch
Institut für Theoretische Elektrotechnik, Gottfried Wilhelm Leibniz Universität, Hannover, Germany
Werner John
System Integration Laboratory GmbH, Paderborn, Germany, and
Wolfgang Mathis
Institut für Theoretische Elektrotechnik, Gottfried Wilhelm Leibniz Universität, Hannover, Germany

Abstract

Purpose – The purpose of this paper is to present an optimization process for the design of a 2×2 patch antenna phased array with application for an UHF RFID system.

Design/methodology/approach – The optimization process is based on a method of moment (MoM)-solver, which was individually made to create such patch antenna phased arrays and simulate the radiated field pattern. In combination with this MoM-solver, a GUI, which gives the opportunity to change every physical antenna factor and create the antenna structure within a few minutes is presented. Furthermore the golden section search method is used to produce an even better solution in a more efficient way compared to the first attempt. After the simulation, different types of presentation of results can be chosen for a fast and easy optimization.

Findings – The design process is discussed while the authors try to optimize the distance between the elements and the difference of input phase for each patch element. The final goal is to create an antenna with maximum directivity and coverage of field pattern.

Practical implications – A physical implementation of an optimized patch antenna phased array and the results of measurement are presented in the end.

Originality/value – An optimization process for the design of a 2×2 patch antenna phased array with application for an UHF RFID system is presented. Furthermore the golden section search method is combined with the design process to increase the accuracy of the solution and decrease the time effort.

Keywords Optimization, Antenna, Golden section search, Method of moments, Phased array, UHF RFID

Paper type Technical paper

The reported R + D work was carried out in the frame of the BMBF-Project smaRTI (Smart ReUsable Transport Items); the smaRTI project is carried out in the frame of the Efficiency Cluster Logistic Ruhr (part of the Leading-Edge Cluster – High-Tech Strategy for Germany). This particular research was supported by the BMBF (Bundesministerium fuer Bildung und Forschung) of Federal Republic of Germany under Grant 01IC10L10H (Save, flexible detection and localization of UHF-RFID-labels in rough environment). The responsibility for this publication is held by the authors only. In particular the authors thank the R + D Coordinator of smaRTI Application Scenario POST Dr W. John (SIL GmbH (iG)) for his ongoing support regarding the RFID challenges of the postal logistic chain and the related industrial R + D requirements. The authors would also like to thank the reviewers for their comments that helped improve the paper.

COMPEL: The International Journal for Computation and Mathematics in Electrical and Electronic Engineering
Vol. 33 No. 6, 2014
pp. 1847-1862

0332-1649
DOI 10.1108/COMPEL-11-2013-0365

1. Introduction

Due to its high gain and controllability of direction of propagation, patch antenna phased arrays are suitable for UHF RFID applications in logistic industries as well as parking management systems, library book management systems and personal identification systems (Finkenzeller, 2003). Such a phased antenna array is discussed, e.g. in Abbak and Tekin (2009). It consists of four patch antennas and is associated with three Wilkinson couplers (Wilkinson, 1960) which can be seen in Figure 1. The elements use a "microstrip line feed" (Balanis, 2005) and are connected with each other via microstrip lines. The operation frequency has a range of 867 MHz (EU, 2006), while the array antenna has a gain of 12.1 dB and utilizes a phase shifter which switches the main-beam between $\pm 40^{\circ}$, with a half-power beam width (HPBW) of approximately 90°. Such a high gain phased array can be used as a reader antenna of an UHF RFID system to obtain extended reading range and coverage.

In this paper a design and optimization process for aforementioned patch antenna phased array is considered. With this process a patch antenna phased array has been designed with temporal acceleration. The design of such an array is complex due to more parameters which influence the input impedance and the radiation pattern. These parameters are the distance d between the patch elements and the input phase difference P between ports 1, 2 (left side) and ports 3, 4 (right side) (Figure 1).

Due to the complex structure of the phased array, the analytical calculation of the radiation fields is impossible. Therefore the antenna problem is solved numerically, while there are many solving methods for patch arrays, which are well suitable for this problem. The method of Skrivervic and Mosig (1992) is based on a convolution technique which yields the finite array characteristics from that of an infinite one. It is capable to solve large patch arrays without any influence on the computer time or memory requirement. Another approach is made by Jandhyala *et al.* (1999) with a fast algorithm with steepest descent fast-multipole method, which can solve large-scale finite microstrip array problems both rapidly and accurately. Due to the small size of the 2×2 array considered in this paper a classic method of moment (MoM)-solver which is a so called 2.5-D simulation is used to calculate antenna properties which will be discussed to find the optimal parameters for d and P. We have implemented our own

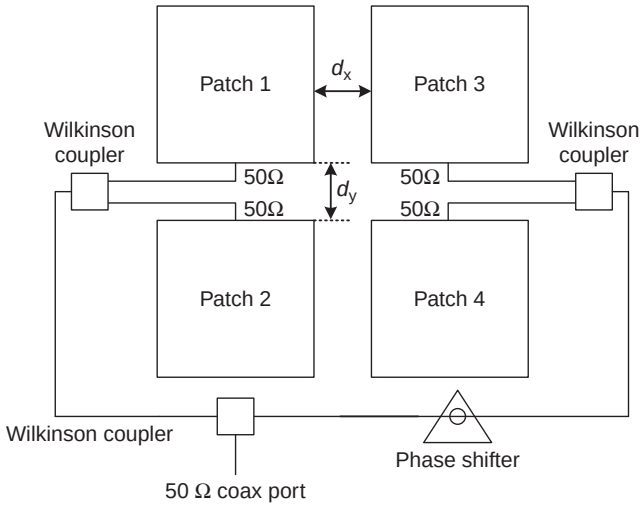

Figure 1.
A simplified sketch of a phased array

design system for the following reasons. First of all a "2.5-D" simulation which is faster than a fully 3-D simulation and sufficient for the design of conventional patch antennas (Coburn *et al.*, 2007) is easy to implement. Second reason is, that the used "golden section search" optimization method, which is one of the most efficient methods for handling one-dimension unimodal problems (Bandler, 1969) has not been found in any commercial 3-D simulation software. Furthermore, an individual GUI can also accelerate a straightforward design process due to the enhanced overview of relevant parameters for modelling and optimizing patch antenna phased arrays.

The paper is organized as follows. In Section 2, the classic MoM-solver is introduced, which is used for the optimization process. In addition the GUI for design process is shown. In Section 3, the detailed design process is described, while in Section 4, the golden section search method is used for a better solution with fewer calculation steps. Manufacture and measurement of this array is shown in Section 5.

2. MoM-solver and GUI

In this section a MoM-solver, which is suitable to calculate the scattered electric field of a perfect electric conductor (PEC) by solving the electric field integral equation will be presented. Based on Rao *et al.* (1982) and Makarov (2002), a set of basis functions will be introduced to approximate the surface current and calculate the impedance matrix.

2.1 MoM-solver

The scattered electric field $\mathbf{E}^s$ of an open or closed conducting body with surface S can be described by:

$$\mathbf{E}^s = -j\omega\mathbf{A} - \nabla\Phi \tag{1}$$

with vector potential:

$$\mathbf{A}(\mathbf{r}) = \mu \int \mathbf{J}(\mathbf{r}') \frac{e^{-jkR}}{4\pi R} \mathrm{d}^3\mathbf{r}' \tag{2}$$

and electric scalar potential:

$$\Phi(\mathbf{r}) = \frac{1}{\varepsilon} \int \sigma(\mathbf{r}') \frac{e^{-jkR}}{4\pi R} \mathrm{d}^3\mathbf{r}' \tag{3}$$

where the spacing between observation point $\mathbf{r}$ and source point $\mathbf{r}'$ is given by $\boldsymbol{R} = |\mathbf{r} - \mathbf{r}'|$ with respect to a global coordinate system with origin O. The charge density σ is given by the equation of continuity:

$$\sigma = \frac{-1}{\mathrm{j}\omega} \nabla \cdot \mathbf{J} \tag{4}$$

and the relation between impressed electric field $\mathbf{E}^i$ and scattered electric field $\mathbf{E}^s$ is defined on the surface S by:

$$\mathbf{n} \times \mathbf{E}^s = -\mathbf{n} \times \mathbf{E}^i \tag{5}$$

It can be seen that the scattered field $\mathbf{E}^s$ depends on the unknown charge density σ and surface current $\mathbf{J}$ and is defined by retarded potential integrals. While the wave number $k = \omega\sqrt{\mu\varepsilon} = 2\pi/\lambda$ contains the time dependence of the wave, the material parameters of the observed space are given by permeability μ and permittivity ε. Assuming that the materials are PECs, the electric field boundary condition can be enforced by $\hat{\mathbf{n}} \times (\mathbf{E}^i + \mathbf{E}^s) = \mathbf{0}$, while $\hat{\mathbf{n}}$ is defined as the normal vector with respect to the antenna surface.

To analyse the antenna structure inside an arbitrary impressed field, it is necessary to take into account the antenna as well as the scatterer (Harrington, 1993). In that content, the antenna is defined as a structure with a source on its surface and the scatterer is defined as a structure with a source in a distance from its surface. After triangulation of the antenna surface we can approximate the surface current by using Rao-Wilton-Glisson (RWG) basis functions described with Equation (6), which are defined on a pair of triangles (Figure 2) (Rao *et al.*, 1982):

$$\mathbf{f}_{\mathrm{n}}(\mathbf{r}) = \begin{cases} \left(\frac{l_n}{2A_n^+}\right)\boldsymbol{\rho}_n^+(\mathbf{r}) & \text{if } \mathbf{r} \text{ in } T_n^+ \\ \left(\frac{l_n}{2A_n^-}\right)\boldsymbol{\rho}_n^-(\mathbf{r}) & \text{if } \mathbf{r} \text{ in } T_n^- \\ 0 & \text{otherwise} \end{cases} \tag{6}$$

Each pair of triangles is defined by triangle T_n^+ and T_n^- which share an interior edge with length l_n and which have the surface area $A_{\overline{n}}^{\pm}$. The basis function is only defined on a pair of triangles correlating to their edge and disappears everywhere else. Introducing a convention on the current direction we define the positive current direction from T^+ to T^-. Due the definition of the basis functions on the edges of the discretized surface, it is necessary to identify all interior basis functions. The surface current $\mathbf{J}$ is given by superposition of a set of basis functions $\mathbf{f_n}$ and complex coefficients i_n such as:

$$\mathbf{J} = \sum_{n=1}^{M} i_n \mathbf{f_n} \tag{7}$$

Devising the $N \times N$ linear equation system where N is the number of basis functions, we can calculate the complex coefficients i_n via:

$$[Z][I] = [U] \quad \text{with} \quad [I] = \begin{bmatrix} i_1 \\ \vdots \\ i_n \end{bmatrix} \quad \text{and}$$
$$[U] = \begin{bmatrix} E_1 \Delta l_1 \\ \vdots \\ E_n \Delta l_n \end{bmatrix} \cdot [Z][I] = [U] \tag{8}$$

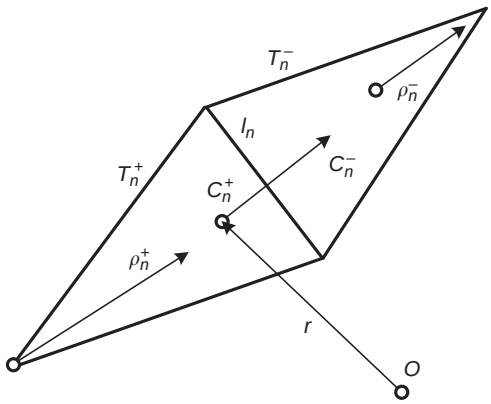

Figure 2.
RWG edge element

Deriving Z from Equation (8) we receive the impedance matrix entries. With Equations (1)-(4) we can calculate the impedance matrix via:

$$Z_{mn} = l_m \left[j\omega \left(\mathbf{A}^{+}_{\mathbf{mn}} \frac{\rho^{\mathbf{C}^{+}}_{\mathbf{m}}}{2} + \mathbf{A}^{-}_{\mathbf{mn}} \frac{\rho^{\mathbf{C}^{-}}_{\mathbf{m}}}{2} \right) + \Phi^{-}_{mn} - \Phi^{+}_{mn} \right] \tag{9}$$

Taking the finite dielectric slab into account we used the solution developed by Newman and Tulyathan (1981). The dielectric slab is replaced by volume polarization currents, where $\mathbf{J}$ is calculated with:

$$\mathbf{J} = j\omega\varepsilon(\varepsilon_R - 1)\mathbf{E} \tag{10}$$

with vacuum permittivity ε and relative permittivity ε_R and:

$$\mathbf{E} = \hat{\mathbf{z}} \frac{1}{2\varepsilon} (\rho_S^{+} - \rho_S^{-}) \tag{11}$$

where $\rho_S^{\pm}$ is the surface charge density on the ground plane and patch and $\hat{\mathbf{z}}$ is the direction of electric field. After solving the equation system, the surface currents can be used to calculate field pattern, input impedance, S_{11} and other desired parameters.

The computational effort for the calculation of impedance matrix and solving of the equation system can be shown on the base of some averaged calculations on a 64-bit Unix System[1] with MATLAB[2]. The calculation of a 2×2 patch array structure takes around 20 minutes, while for a sufficient representation of details 11,500 edges are needed, which correlates to a fully occupied equation system with 11,500 equations and the same number of unknowns.

2.2 GUI

The GUI was designed to provide an environment for a fast design of patch antenna array using the MoM-solver, mentioned above. It consists of an area for geometrical design (Figure 3) and another area for the setup of calculations and the results (Figure 4).

The geometrical design is based on a mesh generator, which is specified for patch antennas. This mesh generator produces a two-dimensional surface mesh using the Delaunay-Triangulation (Delaunay, 1934) which is partly structured. It creates a planar structure for the ground plane and another planar structure for the patch that gets moved in z-direction into the third dimension. On the assumption that the structure is an open PEC body, there is no need to determine an antenna thickness or material parameters. Other antenna properties such as two-dimensional antenna geometry, patch distance to ground plane or discretization size can be set to investigate the radiation behaviour. Furthermore, the number of array antennas, their position and the sequence of feeding can be determined. Alternatively, commercial and non-commercial surface mesh generator, e.g. "Matlab PDE toolbox", "Gmsh" or "GiD" can be used to create geometries similar to the implemented mesh generator. Since there is no need of grouping specific parts of the geometry, there is no high requirement in the complexity of the mesh generation programme. The mesh information can get imported into MATLAB with the most common mesh formats IDES, STL, MSH, STEP or BRep. After the antenna structure has been created, the feeding edge will be identified at the first inner edge of the feeding line that represents the strip line (Makarov, 2002). The advantage of this environment is the possibility to set every single parameter that will influence the radiation properties of the antenna.

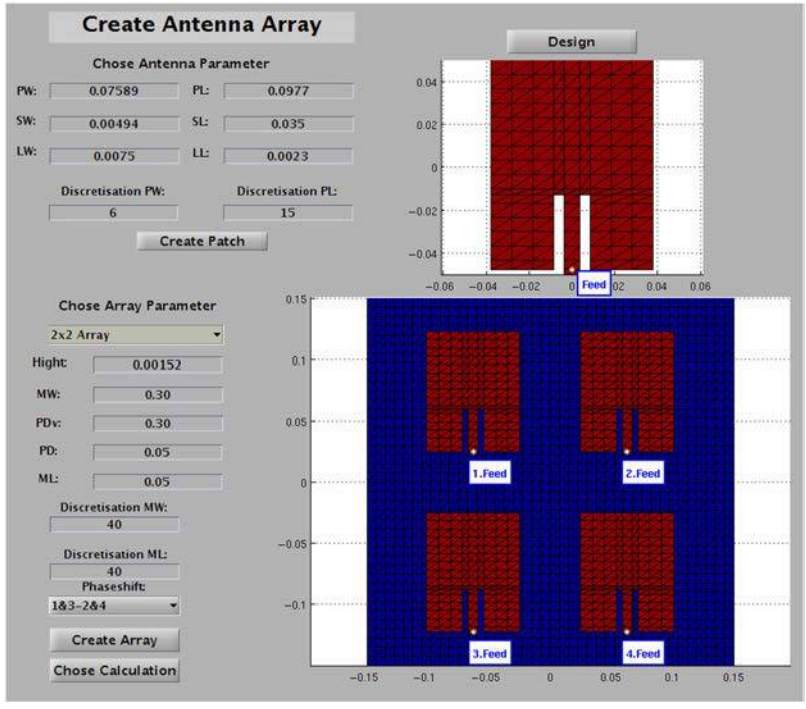

Figure 3.
Design area of the solver

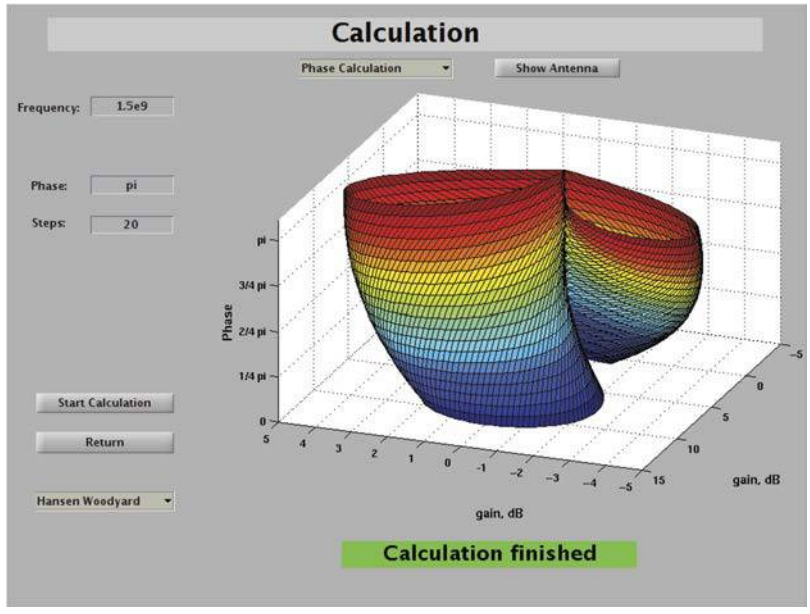

Figure 4.
Calculation area of the solver

After defining the antenna parameters, the calculation can be set up. It is possible to choose between a simple field calculation and a set of loop calculations. The fastest operation is a single field calculation of the created antenna for which the described MoM-solver calculates the radiation properties for a given frequency and phase. Over a given frequency range and a number of calculation steps, it is possible to calculate the trend of return loss in that range. Another loop calculation can be made to investigate the phase behaviour of the antenna. Apart from defining a frequency, a phase range and a number of calculation steps can be set. The last selectable process is the distance calculation, for which preferences for the frequency, the phase and the respective vertical and horizontal distance ranges must be set.

Different presentation possibilities of the results including antenna gain, main beam orientation and HPBW pointing out a conclusion about antenna properties for an optimal radiation behaviour. Apart from the Hansen-Woodyard Model (Figure 4) the results can be represented via a polar diagram, a 2D plot of curves, a smith chart or a sphere plot in which the radiated energy is projected onto a triangulated sphere surface (Makarov, 2002). Additionally investigations about the influence of discretization on the result and the stability of the solver can be investigated.

3. Array design

In this section, a design process is presented for the patch antenna phased array (Figure 1), using the aforementioned solver and GUI. This 2×2 array consists of four antenna elements while each array element was designed according to Balanis (2005). This element has a maximal directivity D_{max} of 5 dBi and a HPBW of 92.7° at 867 MHz. The properties of that elements stay unaltered during further design process. To get an optimal array there are three goals to achieve:

(1) $S_{11} \leqslant -10$ dB at 867 MHz.

(2) The maximum antenna directivity D_{max} should be as high as possible.

(3) The angular range, that covers all points with condition directivity $D > 5$ dBi (maximum directivity of a single patch antenna), should be as wide as possible if the second goal is archived.

To achieve the three goals, the S_{11}-parameter and the radiation pattern should be investigated during the adjustment of the physical factors. The alterable physical factors of the array are the distances between the elements in x- and y-directions d_x, d_y (Figure 1) and the phase difference P between the elements. The feeding circuit in Figure 1 is not considered for investigation in order to keep the model simple and the simulation fast.

We vary the physical factors with small steps in a predefined range and operate a separate simulation for each step. By changing only one parameter all the others are kept unchanged. This method ensures that the considered antenna property is not influenced by another physical factor. The results of all the simulations will be combined in a single diagram to make it possible to have an overview about the trend of the parameters over the total sweep range of the physical factors. At the end we choose the optimal results from the investigation and use them on the final model. As quality criteria for choosing optimal results, the simulation results themselves as well as the physical applicability of array dimensions are respected.

3.1 Investigation by varying element spacing

The two distances d_x and d_y are investigated separately. First of all d_y is analysed in a range of $0.04\,\lambda$[3] to λ while $d_x = 0.5\lambda$ and the phase shift is set to $P = 0°$. Due to the

periodicity of waves, a simulation for $d_y \geqslant \lambda$ is not necessary. Every variation of d_y causes a new simulation, while the results of S_{11}-parameter and the maximum directivity D_{max} are investigated. The starting value $d_x = 0.5\lambda$ was determined according to an investigation of an 2 × 2 isotropic source array. If a plane wave of λ wavelength impinges on an arbitrary planar array with N isotropic elements in (ϕ,θ) direction where θ and ϕ denote the azimuth and polar angles, the array beam pattern in far-field are defined by (Van Trees, 2002):

$$G_{iso}(\phi, \theta) = \sum_{i=1}^{N} w_i e^{-j\frac{2\pi}{\lambda}(u_x x_i + u_y y_i)} \tag{12}$$

in direction $u_x = \sin\theta \cos\phi$ and $u_y = \sin\theta \sin\phi$ with $0 \leqslant \phi < 2\pi, 0 \leqslant \theta < \pi$. w_i is the complex weight and (x_i, y_i) is the position of the ith element. In order to consider the far-field radiation pattern of the patch antenna, the element factor EF is taken into account. The relationship is given in Gross (2005) as $G(\phi,\theta) = EF \times AF$. AF is the array factor which equals G_{iso} in Equation (12). The array factor EF of a patch-antenna forms a single main lobe while its maximum points in the normal direction with $\theta = 0$. Due to its linear relationships with EF the maximum array gain $G_{max}(\phi,\theta)$ depends only on AF by a phase shift of $P = 0°$. Figure 5 shows the ratio between the maximum directivity D_{max} of an 2 × 2 isotropic source array with element spacings d_x, d_y. A maximum is achieved at approximately $d_x = d_y = 0.8\lambda$. Due to the U-shaped trend in Figure 5 we can reach the global maximum in two steps:

(1) choose d_x ($d_x > 0.5$) as start value and run simulation by varying d_y (the blue line parallel to d_y-axis in Figure 5); and

(2) choose d_y value with maximal value from step 1 and rerun the simulation by varying d_x to reach the global maximum directivity (the blue line parallel to d_x-axis in Figure 5).

The results of S_{11}-parameter are shown in Figure 6. The first goal $S_{11} \leqslant -10$ dB is satisfied in the total range of d_y. The ratio between D_{max} and d_y is described in Figure 7. Starting with a global minimum of 10.5 dBi the parameter D_{max} increases in a uniform manner until it reaches its maximum with 13.7 dBi at $d_y = 0.42\lambda$. Once it reaches its maximum, D_{max} decreases until it reaches a local minimum with 11.3 dBi at $d_y = 0.9\,\lambda$.

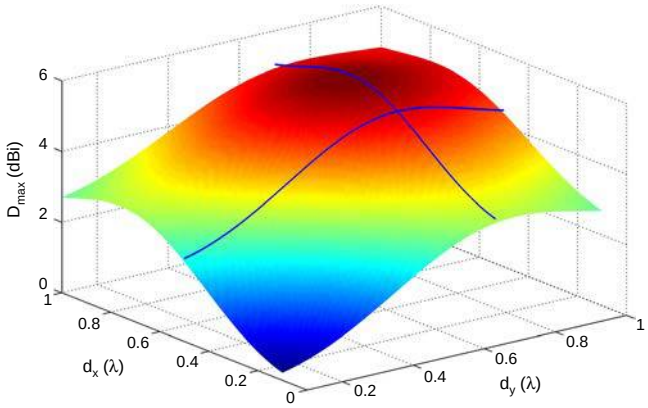

Figure 5.
D_{max} with varied d_x and d_y (isotropic source array)

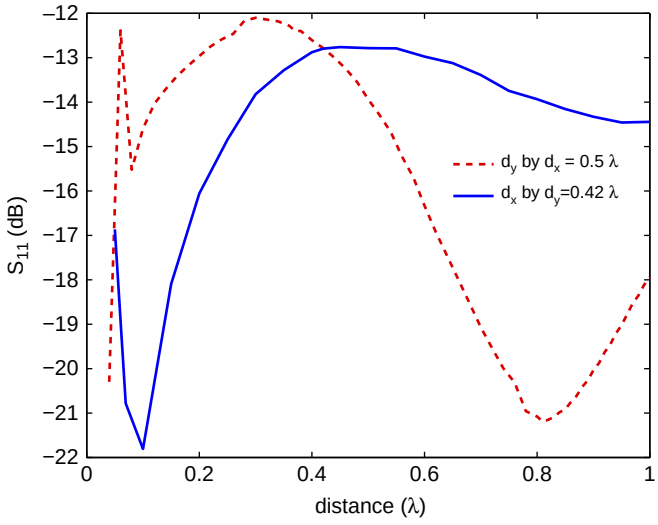

Figure 6.
S_{11} over distances of elements

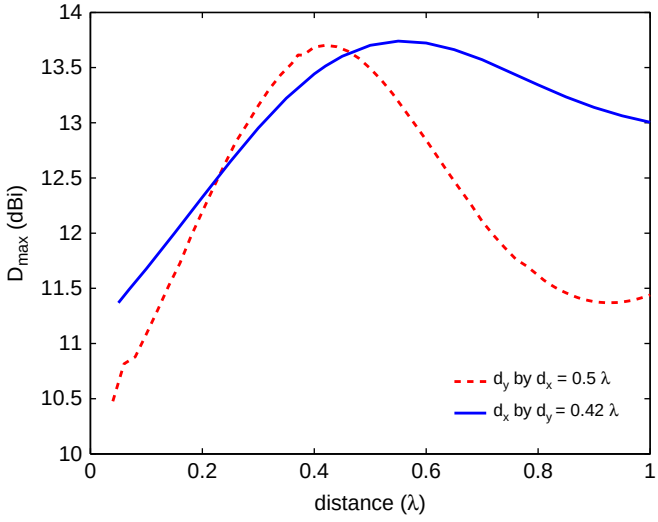

Figure 7.
Directivity over distances of elements

In the following investigations, the first optimized parameter $d_y = 0.42\,\lambda$ is set as optimized distance in the y-direction.

For the second investigation, d_x gets analysed in a range of $0.05\,\lambda$ to λ while $d_y = 0.42\,\lambda$ and the phase shift is set to $P = 0°$. Equivalent to the analysis of the influence of d_y on S_{11}-parameter and maximum directivity D_{max}, d_x gets investigated. The results of the S_{11}-parameter are shown in Figure 6. The first goal $S_{11} \leqslant -10$ dB is satisfied in the total range of d_x. The ratio between D_{max} and d_x is described in Figure 7. Starting with a global minimum of 11.4 dBi the parameter D_{max} increases uniformly until it reaches its maximum with 13.7 dBi at $d_x = 0.55\,\lambda$. Once it reaches its maximum, D_{max} decreases until it reaches a local minimum of 13 dBi at $d_x = \lambda$. In the following investigations, the second optimized parameter $d_x = 0.55\,\lambda$ is set as the optimized

distance in the x-direction. The second goal is satisfied by choosing the optimized distances $d_x = 0.55\lambda$ and $d_y = 0.42\lambda$, which are used for the further investigation.

3.2 Investigation by varying phase of port

As described in Figure 1, a phase shifter for port 3 and 4 is build-in the array while port 1 and 2 (left side) and port 3 and 4 (right side) are in phase. The orientation of main beam by phase $P = 0^\circ$ for all ports is aligned in positive z-direction. The phase difference P between the ports 1, 2 and the ports 3, 4 is caused by the phase shifter, which enables a change of orientation of the main beam in xz-plane in a specific angle range.

In this investigation we change the phase difference P between -180° and 180°. While simulating, the changes of the S_{11}-parameter, the vertical alignment of the main beam ϑ_D and D_{max} will be considered.

Starting with a global minimum of 11.1 dBi at $P = \pm 180^\circ$ the parameter D_{max} increases in a uniform manner until it reaches its maximum with 13.7 dBi at $P = 0^\circ$ (Figure 8). Once it reaches its maximum, D_{max} decreases until it reaches a local minimum with 11.1 dBi at $P = 180^\circ$. It can be seen that D_{max} behaves axis symmetrically in dependence of phase difference P and has the form of a parabola.

The orientation of main beam ϑ_D has nearly a linear course between $\pm 28^\circ$ in the range of $P = \pm 170^\circ$ (Figure 8). Special cases are the values at $P = \pm 180^\circ$. The jump between the maximum at $P = -180^\circ$ with 29° and the minimum at $P = 180^\circ$ with -29° can be explained with the polar diagram of Figure 9. This diagram shows the radiation pattern of the antenna at $P = -180^\circ$ and 180° It can be seen that there are two axis symmetric main beams in the range of $|P| \geqslant 170^\circ$ resulting in a small difference between the two diagrams. Depending in which direction the phase $|P|$ will be changed one of the symmetric main beams will increase while the other will decrease. At this point the curve in Figure 8 will either jump up or down.

On the basis of a slow change of $\vartheta_{D_{max}}$ with respect to P, we get a large angle range of P for an optimal phase array. As shown in Figures 10 and 11, both polar diagrams have nearly the same angle range at $P = \pm 60^\circ$, respectively, $P = \pm 90^\circ$ with 127° that covers all the points with directivity $D \geqslant 5$ dBi. Furthermore both phase-shift diagrams have no zero. The array has a directivity of $D = 12.35$ dBi at $\vartheta = 0^\circ$ with phase $P = \pm 60^\circ$ whereas there is only a directivity of $D = 10.57$ dBi at phase $P = \pm 90^\circ$. There is a directivity of $D = 7.7$ dBi at $\vartheta = \pm 35^\circ$ with phase $P = \pm 90^\circ$ whereas there is

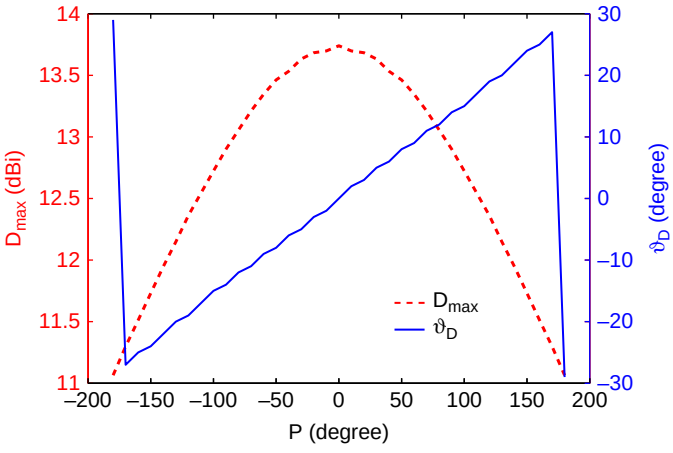

Figure 8.
Directivity D_{max} and main beam direction ϑ_D over phase difference P

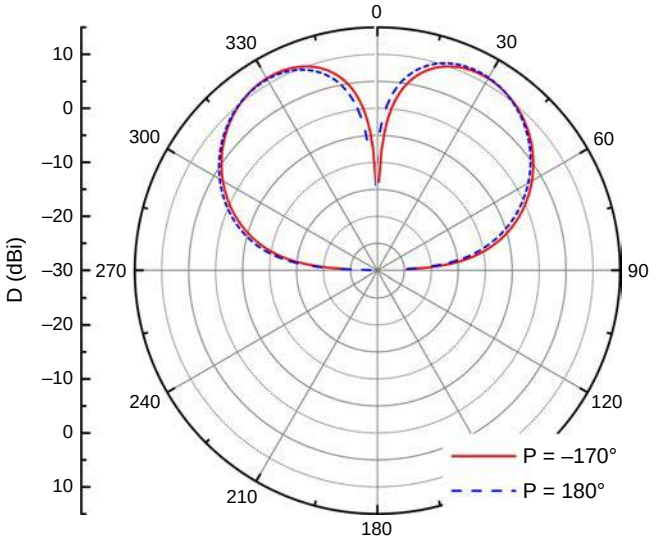

Figure 9.
Directivity pattern by $P = 170^\circ$ and -180° ($\phi = 0^\circ$)

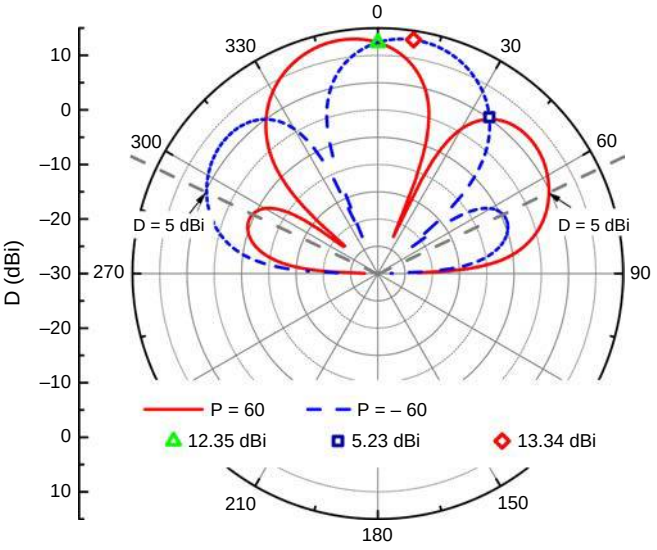

Figure 10.
Directivity pattern by $P = \pm 60^\circ$ ($\phi = 0^\circ$)

only a directivity of $D = 5.2$ dBi with phase $P = \pm 60^\circ$. The value for D_{max} is 13.34 dBi at $\vartheta = 9^\circ$ with $P = \pm 60^\circ$ and 12.89 dBi at $\vartheta = 14^\circ$ with $P = \pm 90^\circ$.

Another advantage of a small P is that there is less need of spacing for the phase shifter. It is possible to see that the third condition is satisfied by achieving a total angular range of 127°, that covers all the points with condition directivity $D >$ dBi (Figure 10).

4. Optimization

The method shown above, which was used to find the optimal parameters for d_x and d_y, is capable to perform that task but still needs several simulation steps. The method collects all simulation results, calculated in a fixed number of uni-distant steps, to find

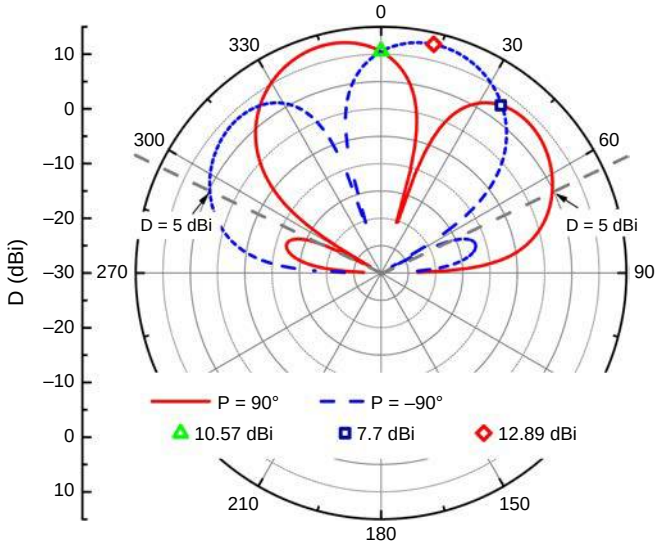

Figure 11.
Directivity pattern by $P = \pm 90^{\circ}$ ($\phi = 0^{\circ}$)

the maximum parameter by comparing all the results at once in the end. Because the result progression shown in Figures 6 and 7 indicates an optimum solution in the unimodal interval from 0.2 to 0.8 λ, the golden section search method, based on Kiefer (1953) and Avriel and Wilde (1968) is used in order to perform a better solution with less simulation steps for d_x and d_y. Since the number of simulation steps is unknown at the beginning of the simulation, this method is one of the most effective minimax direct elimination methods (Bandler, 1969). The method investigates simulation results with each step to calculate, in dependence of that, the next step for d_x or d_y. The only condition the simulation data has to satisfy is that it can be represented by a unimodal continuous function. As long as this condition is satisfied the algorithm will not fail.

4.1 Optimization algorithm

The input for the algorithm comprises an interval $[a,b]$ in which the maximum is assumed, an abort criterion ε and a maximum number of steps N, which will be used to stop the algorithm if either the solution is close enough to the real one or the algorithm exceeds N. The initial values are calculated with:

$$x_1 = c \cdot a + (1 - c) \cdot b \tag{13}$$

$$x_2 = (1 - c) \cdot a + c \cdot b \tag{14}$$

while $c = \left(-1 + \sqrt{5}\right)/2 \approx 0.618$, which is the golden ratio (Bandler, 1969). Let $f(x_i)$ be the simulation result with x_i, there can be two possible cases which give an interval reduction with:

$$f(x_1) < f(x_2) \begin{cases} x_{1,new} = x_2 \\ x_{2,new} = (1 - c) \cdot x_1 + c \cdot x_2 \end{cases} \tag{15}$$

$$f(x_1) > f(x_2) \begin{cases} x_{1,new} = c \cdot x_1 + (1 - c) \cdot x_2 \\ x_{2,new} = x_1 \end{cases} \tag{16}$$

The new interval is $[x_1, x_2] = [x_{1,new}, x_{2,new}]$, which includes only one new simulation step. The algorithm repeats itself until the abort criterion with:

$$|x_1 - x_2| \leqslant \varepsilon \tag{17}$$

is satisfied or the number of iterations exceeds N. The final solution is given by x_1 with $f(x_1)$ if the last iteration step was with case $f(x_1) > f(x_2)$ and vice versa.

4.2 Optimized investigation by varying element spacing

To show the efficiency of the golden section search method, we use it for the optimization process of distance d_y with fixed d_x value of 0.5 λ. By comparing the results with previous calculated results with uni-distant steps we can evaluate the algorithm.

As shown in Figure 12 there is a fast convergence of the algorithm, since 72 percent of the simulations are very close the final solution. Furthermore we find an optimum solution after 11 varied simulation steps with an accuracy of $\varepsilon = 0.01$. Compared with the previous calculations, for which we needed 31 uni-distant steps, we save approximately two-thirds of simulation run-time.

5. Manufacture and measurement

As part of the design process, a 2 × 2 antenna array has been manufactured in consideration of optimizing the results. The used substrate is FR-4 with a relative permittivity $\varepsilon_r = 4.3$. Due to the maximal size of such a substrate plate, the implement ability of optimized parameters is limited. Because of that an agreement had to be made with the values of distance d_x and d_y between the patch elements. Three identical Wilkinson power dividers for 50 Ω port impedance and 867 MHz were made according to Wilkinson (1960). In addition, a phase shifter with a fixed shifting rate of 60° has been implemented consulting (Nakada *et al.*, 2000). It consists of two separate microstrip lines which are switchable with two HF-SPDT switches. The switch procedures are controlled by 5V DC power-supply source.

The antenna array and its installation of measurement for S_{11}-parameter are shown in Figure 13. Figure 14 shows the measured S_{11}-parameter. Moreover the array matches its first resonance for 50 Ω at 867 MHz and reaches a S_{11} of −21 dB.

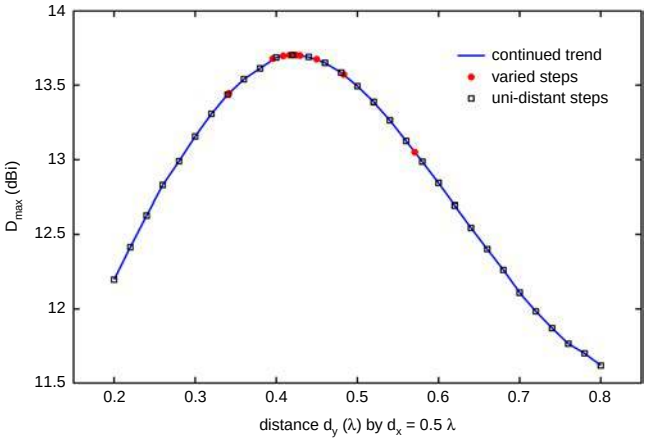

Figure 12.
Directivity over distances of elements with optimized algorithm

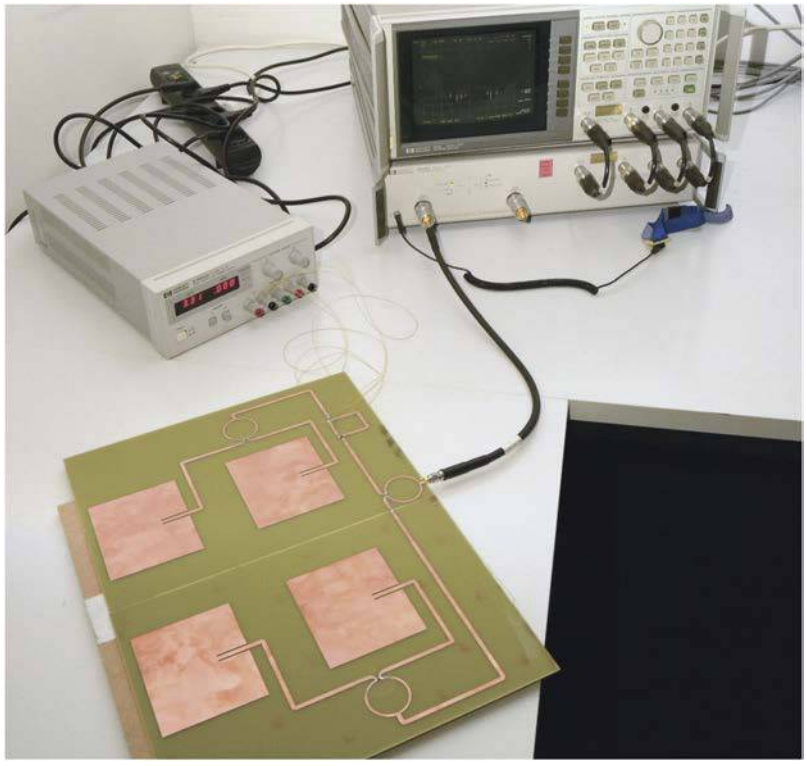

Figure 13.
Measurement of the 2 × 2 antenna array

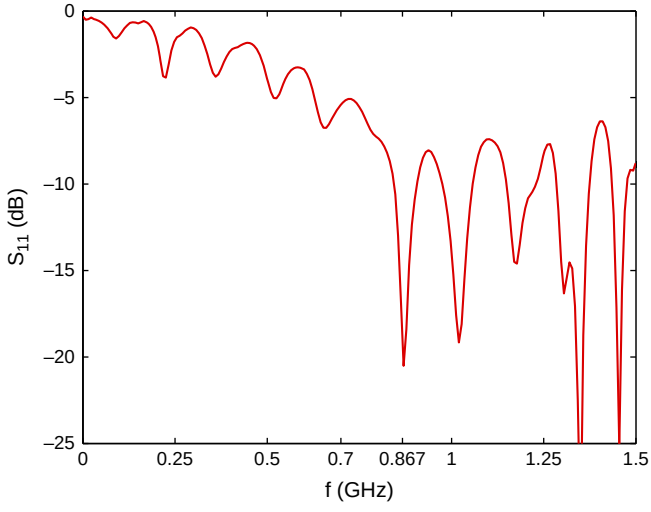

Figure 14.
S_{11} of measurement

6. Conclusion

A MoM-solver combined with an optimization algorithm and individual GUI for a fast design of 2×2 patch antenna phased arrays has been presented. The complete design process of such phased patch array has been discussed, while there are only three physical factors to consider. These are the distances of the elements d_x, d_y and the difference of input phase for each patch element P. According to the results of simulation we calculated the optimized values for distance $d_x = 0.55\,\lambda$ and $d_y = 0.42\,\lambda$. The ideal difference of input phase between ports 1, 2 and 3, 4 of the elements is in the range $60^\circ \leqslant |P| \leqslant 90^\circ$. With these optimized values we get optimal antenna properties on the desired frequency band, which are $S_{11} \leqslant 10$ dB, maximum directivity $D_{max} =$ 13.7 dBi at $P = 0^\circ$ and maximum angular range of the main beam of about 127° at $\phi = 0^\circ$. By introducing an optimization algorithm we could decrease the time effort by approximately 66 percent.

Notes

1. Intel Core i5-3210M with $4 \times 2.5\,GHz$ and $8\,GB$ RAM.
2. MATLAB 7.11.0 R2010b.
3. Microstrip line uses $0.04\,\lambda$ in y-direction.

References

Abbak, M. and Tekin, I. (2009), "RFID coverage extension using microstrip-patch antenna array (wireless corner)", *IEEE Antennas and Propagation Magazine*, Vol. 51 No. 1, pp. 185-191.

Avriel, M. and Wilde, D.J. (1968), "Golden block search for the maximum of unimodal functions", *Management Science*, Vol. 14 No. 5, pp. 307-319.

Balanis, C.A. (2005), *Antenna Theory: Analysis and Design*, 3rd ed., Wiley-Interscience, Markham.

Bandler, J.W. (1969), "Optimization methods for computer-aided design", *IEEE Transactions on Microwave Theory and Techniques*, Vol. 17 No. 8, pp. 533-552.

Coburn, W.O., Ly, C. and Weiss, S. (2007), "Patch antenna modeling issues using commercial software", *IEEE International Symposium on Electromagnetic Compatibility EMC 2007*, pp. 1-7, available at: http://ieeexplore.ieee.org/xpl/articleDetails.jsp?tp=&arnumber=4305608&queryText%3DPatch+antenna+modeling+issues+using+commercial +software%E2%80%9D%2C+IEEE+International+Symposium+on+Electromagnetic+Compatibility+EMC+2007.

Delaunay, B. (1934), *Sur La Sphère Vide*, A la mémoire de Georges Voronoï, Bulletin de l'Académie des Sciences de l'URSS. Classe des sciences mathématiques et na, No. 6, pp. 793-800.

EU (2006), "Commission decision of 23. November 2006 on harmonisation of the radio spectrum for radio frequency identification (RFID) devices operating in the ultra-high frequency (UHF) band (notified under document number C(2006) 5599) (2006/804/EC)", EU.

Finkenzeller, K. (2003), *RFID Handbook: Fundamentals and Applications in Contactless Smart Cards and Identification*, 2nd ed., John Wiley & Sons Inc., New York, NY.

Gross, F.B. (2005), *Smart Antennas for Wireless Communications: With MATLAB (Professional Engineering)*, McGraw-Hill, New York, NY.

Harrington, R.F. (1996), *Field Computation by Moment Methods*, Wiley-IEEE Press, Hoboken.

Jandhyala, V., Michielssen, E., Shanker, B. and Chew, W.C. (1999), "A fast algorithm for the analysis of radiation and scattering from microstrip arrays on finite substrates", *Microwave and Optical Technology Letters*, Vol. 23 No. 5, pp. 306-310.

Kiefer, J. (1953), "Sequential minimax search for a maximum", *Proceedings of the American Mathematical Society, Proc. Amer. Math. Soc. 4, Department of Mathematical Statistics at Columbia University, New York, NY*, pp. 502-506.

Makarov, S. (2002), *Antenna and EM Modeling with Matlab*, Wiley-Interscience, New York, NY.

Nakada, K., Marumoto, T. and Iwata, R. (2000), "Stub switched phase shifter", *IEEE Antennas and Propagation Society International Symposium 2000*, Vol. 2, pp. 812-815, available at: http://ieeexplore.ieee.org/xpl/articleDetails.jsp?tp = &arnumber = 875337&queryText% 3DStub + Switched + Phase + Shifter

Newman, E.H. and Tulyathan, P. (1981), "Analysis of microstrip antennas using moment methods", *IEEE Transactions on Antennas and Propagation*, Vol. 29 No. 1, pp. 47-53.

Rao, S.M., Wilton, D. and Glisson, A.W. (1982), "Electromagnetic scattering by surfaces of arbitrary shape", *IEEE Transactions on Antennas and Propagation*, Vol. 30 No. 3, pp. 409-418.

Skrivervic, A.K. and Mosig, J.R. (1992), "Finite phased array of microstrip patch antennas: the infinite array approach", *IEEE Transactions on Antennas and Propagation*, Vol. 40 No. 5, pp. 579-582.

Van Trees, H.L. (2002), *Optimum Array Processing (Detection, Estimation, and Modulation Theory, Part IV)*, Wiley-Interscience, Hoboken.

Wilkinson, E.J. (1960), "An N-way hybrid power divider", *IRE Transactions on Microwave Theory and Techniques*, Vol. 8 No. 1, pp. 116-118.

Corresponding author
Yuanhao Wang can be contacted at: ywang@tet.uni-hannover.de